Antiresonant Reflecting Optical Waveguide Surface Plasmon Resonance Sensors

Yang-Tung Huang, Wei-Zung Chang, Shih-Hsin Hsu, Chun-Ho Chen and Jou-Chien Chen
Department of Electronics Engineering and Institute of Electronics
National Chiao Tung University
1001 Ta-Hsueh Road, Hsinchu, Taiwan, Republic of China
TEL: 886-3-5712121 Ext. 54138
FAX: 886-3-5724361
E-Mail: huangyt@cc.nctu.edu.tw

ABSTRACT

An ARROW-B (antiresonant reflecting optical waveguide, type B) surface plasmon resonance (SPR) sensor operating in aqueous environment is proposed. The characteristics, design, and optimization of the Au-coated ARROW-B SPR sensor are discussed. The operating range of the sensor can be shifted by adding a dielectric overlay. The detectable changes of the refractive index down to the order of 10^{-5} can be achieved. The design of an ARROW SPR sensor on Si substrates for detecting hydrogen molecules with palladium as the metal film will also be discussed.

Keywords: waveguide sensors, surface plasmon resonance, antiresonant reflecting optical waveguides

1. INTRODUCTION

Surface plasmon resonance for use in chemical and biochemical sensing has been receiving growing research efforts for the past two decades.[1] Among several kinds of SPR sensor configurations, e.g. prism SPR sensors, grating SPR sensors, fiber SPR sensors, and waveguide SPR sensors, waveguide-based SPR sensors have many attractive features such as compact size, ruggedness, prospect of fabrication of multiple/multichannel sensors on a single chip, etc.[2] In contrast to conventional waveguides, antiresonant reflecting optical waveguides (ARROW's) utilizing antiresonant reflection as guiding mechanism instead of total internal reflection can perform low-loss single mode propagation with relatively large core sizes.[3] Moreover, to support the surface plasmon wave (SPW) which is TM-polarized, a polarization-insensitive ARROW-B waveguide[4] was adopted as the wave-guiding structure.

In this presentation, an ARROW-B (antiresonant reflecting optical waveguide, type B) surface plasmon resonance (SPR) sensors operating in aqueous environment is proposed. The characteristics of ARROW-B waveguides and surface plasmon waves are investigated. A design example of Au-coated ARROW-B SPR sensors is given. To shift the operating range into the desired environment, a dielectric overlay added onto the metal layer was applied. Finally, the optimization of Au-coated ARROW-B SPR sensors is presented. In addition, the design of an ARROW SPR sensor for detecting H_2 molecules with Pd as the metal film will also be discussed.

2. CHARACTERISTICS OF ARROW-B WAVEGUIDES AND SURFACE PLASMON WAVES

2.1. Characteristics of ARROW-B Waveguides

Since the first demonstration of antiresonant reflecting optical waveguides (ARROW's) was introduced in 1986,[3] there has been increasing research interest in this type of devices. Utilizing antiresonant reflection as waveguiding mechanism instead of total internal reflection, ARROW structures are promising because of many unique features, such as polarization and wavelength selective characteristics, relaxed fabrication tolerance, effective single-mode propagation, low losses, good light confinement, and efficient connection to single mode fibers. As a result that an conventional ARROW can only support low-loss propagation for a single TE-polarized wave and the surface plasmon wave is TM-polarized, another family of ARROW's called ARROW-B,[4] which can support low-loss

Device and Process Technologies for MEMS and Microelectronics II,
Jung-Chih Chiao, Lorenzo Faraone, H. Barry Harrison, Andrei M. Shkel, Editors,
Proceedings of SPIE Vol. 4592 (2001) © 2001 SPIE · 0277-786X/01/$15.00

TM-polarized waves, has to be used. Fig. 1 shows the basic structures and the index profiles of ARROW and ARROW-B. The major difference is the refractive index of the first cladding is higher than that of the core for an conventional ARROW waveguide, while it is lower for an ARROW-B waveguide.

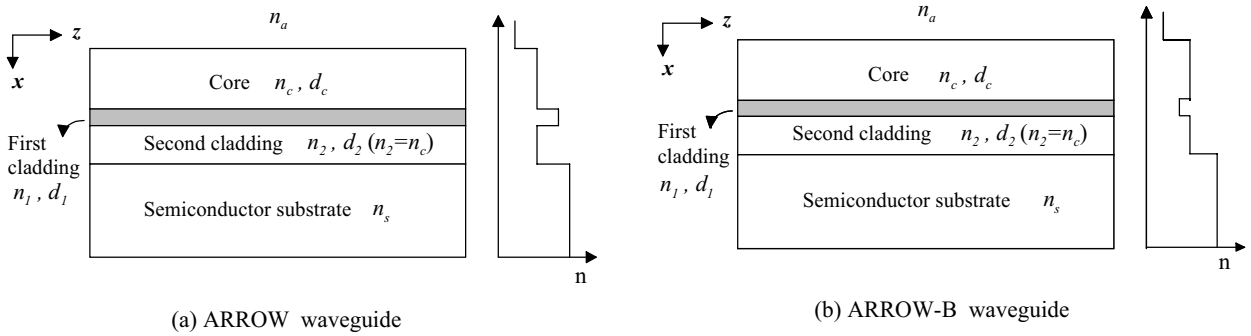

Figure 1. Structures and index profiles of ARROW and ARROW-B.

For an ARROW-B waveguide, the thickness of the second cladding layer is governed by the transverse antiresonant condition as[5]

$$d_2 \simeq \frac{\lambda}{4n_2}\left[1-\left(\frac{n_c}{n_2}\right)^2+\left(\frac{\lambda}{2\,n_2 : d_{ce}}\right)^2\right]^{-1/2}\cdot(2N+1), \qquad (N=0,1,2,\cdots) \tag{1}$$

where d_{ce} is the equivalent thickness of the core. d_{ce} can be approximately given by

$$d_{ce} \simeq d_c + \xi_0 \frac{\lambda}{2\pi\sqrt{n_c^2-n_0^2}} + \xi_1 \frac{\lambda}{2\pi\sqrt{n_c^2-n_1^2}\,\tanh\{(2\pi/\lambda)\,d_1\sqrt{n_c^2-n_1^2}\}}, \tag{2}$$

where

$$\xi_i = \begin{cases} 1 & \text{for TE modes,} \\ \left(\frac{n_i}{n_c}\right)^2 & \text{for TM modes.} \end{cases} \tag{3}$$

Typically, the material of the second cladding layer is chosen as same as that of the core, hence Eq. (1) can be reduced to

$$d_2 \simeq \frac{d_{ce}}{2}(2N+1), \tag{4}$$

and N is designed to be zero in most cases. In order to sustain effectively single-mode and low-loss propagation, the thickness of the first cladding layer d_1 has to be carefully chosen. With a material system of (water/SiO_2/MgF_2/SiO_2/Si) and corresponding refractive indices of (1.332/1.460/1.378/1.460/3.500) at the operating wavelength $\lambda = 0.6328$ μm, $d_1 = 0.27$ μm can be found to be a suitable value for the chosen $d_c = 4.00$ μm and $d_2 = 2.00$ μm.

2.2. Characteristics of Surface Plasmon Waves

A surface plasmon wave is a strongly localized electromagnetic surface wave that propagates along an interface between metallic and dielectric media. For the bound mode which can be guided by the interface, its propagation constant can be expressed as[6]

$$\beta_{\rm sp} = k_0\sqrt{\frac{\epsilon_d\,\epsilon_m}{\epsilon_d+\epsilon_m}}, \tag{5}$$

where k_0 is the freespace wavenumber, and ϵ_d ($= n_d^2$) and ϵ_m are relative permittivities of the dielectric and metal, respectively.

Consider a metal/dielectric interface on top of an optical waveguide. Efficient waveguide-to-plasmon coupling can be obtained if the propagation constant of the surface plasmon wave $\beta_{\rm sp}$ is close to that of the waveguide mode. The closer the two propagation constants are, the higher coupling efficiency will be. The effect of properties of the metal and the dielectric on surface plasmon wave excitation will be clearer in the following discussion.

3. DESIGN OF ARROW-B SPR SENSORS

The basic structure of an ARROW-B SPR sensor shown in Fig. 2 consists of three sections. Sections F_1 and F_2 are the input and output effective single-mode ARROW-B waveguides, and S is the sensing section which supports surface plasmon waves. On top of the waveguide core is a metal thin film, and the length of the sensing region is typically assumed to be 2 mm. Among several metals possessing characteristics of surface plasmon waves,[7] some are not practical for SPR applications and gold (Au) is one of the suitable materials for its stability and inertness.[8]

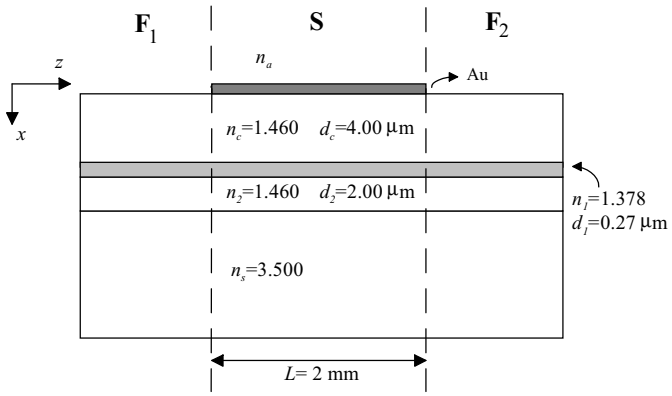

Figure 2. Basic structure of an ARROW-B SPR sensor.

To investigate the effect of the refractive index of the environment (superstrate) on surface plasmon wave excitation, Fig. 3 shows the effective indices of the two lowest-order modes in the sensing section of the Au-coated ARROW-B SPR sensor versus superstrate index n_a. The relative permittivity of gold ϵ_m is assumed to be $-12.200 - 1.300i$ at $\lambda = 0.6328$ μm,[9] and the thickness of gold layer d_m is set to 40 nm.

It's obvious that there is a turning point around $n_a = 1.363$. This turning point represents the maximum coupling efficiency of waveguide-to-plasmon coupling. For the case on the left of the turning point, the quasi-guided modes are pretty similar to ordinary ARROW modes. For the case on the right, however, the fundamental mode of the ARROW-B SPR sensor is no longer an ARROW mode, but a surface plasmon (SP) mode. The modal evolution and transition can also be found by observing the power transmission characteristics.

In regard to the operation of the ARROW-B SPR sensor, when there is a variation in the refractive index of the environment, the field profile of the waveguide mode will change. Consequently, the mode-coupling at the interface and thus the surface plasmon wave excitation will also change. In this case, and the output power through the sensor will be changed which corresponds to the environment index variation. The relative output power through the ARROW-B SPR sensor can be expressed as

$$p(L) = \left| a_0(L)/a_0(0) \right|^2 , \tag{6}$$

where $a_0(0)$ and $a_0(L)$ are the complex amplitudes of the fundamental modes at the input and output of the sensor, respectively.

Fig. 4(a) shows the relative output powers (in unit of dB) versus superstrate index n_a for different thickness of gold layer d_m. The minimum relative output powers correspond to the best resonant coupling from the guide

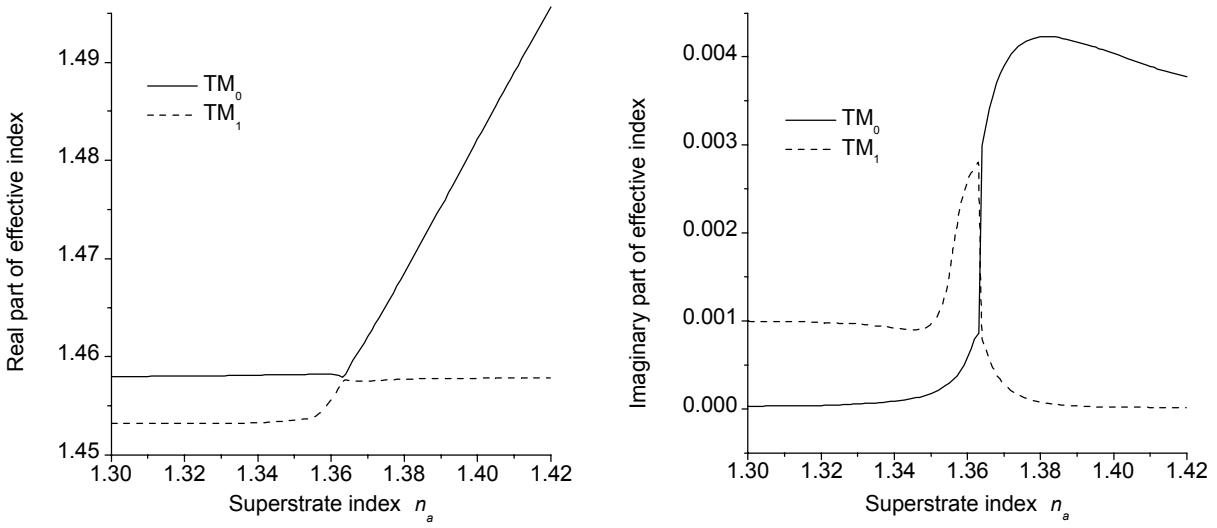

Figure 3. Real and imaginary parts of effective indices of the TM_0 and TM_1 in the sensing section of the ARROW-B SPR sensor.

mode of the ARROW waveguide to the surface plasmon mode. Since the sensitivity of the sensor is proportional to the slope of the relative output power curve, the one which has a steeper slope should be more suitable for high-sensitivity sensing applications. By further comparison as shown in Fig. 4(b), it was found that the curve for $d_m = 35$ nm has the steepest slope on both sides of the valley. As a result, the thickness of the gold layer of the ARROW-B SPR sensors was set to be 35 nm.

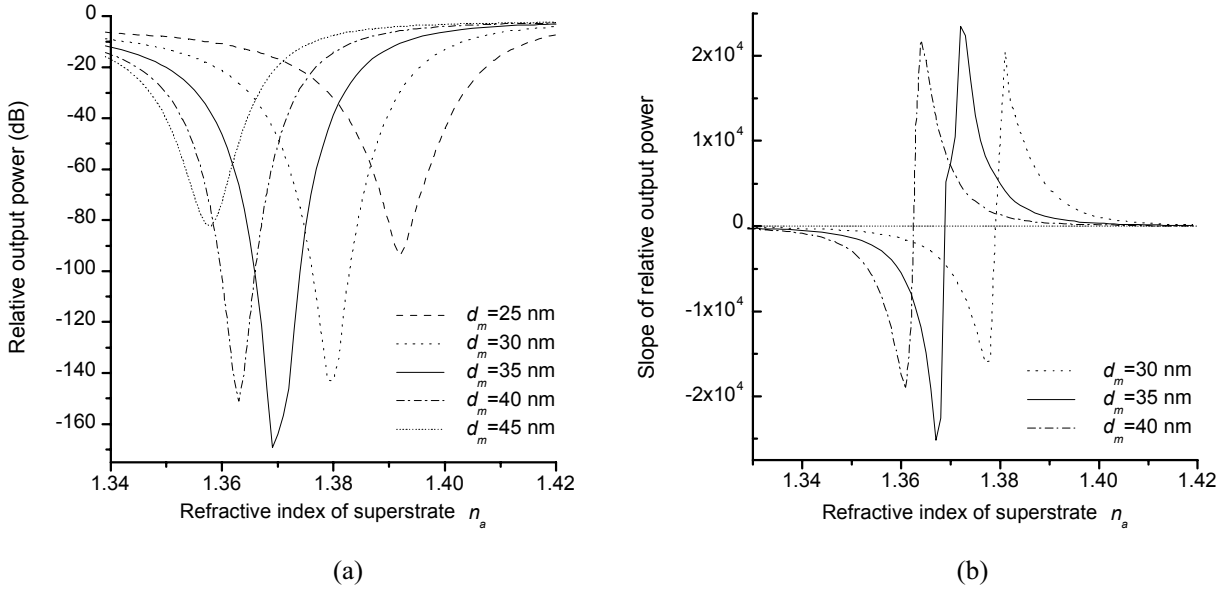

(a) (b)

Figure 4. Dependence of the (a) relative output power and (b) the slope of that on the superstrate index.

4. OVERLAY TUNING AND OPTIMIZATION

Although the ARROW-B SPR sensor presented in the previous section is highly sensitive to superstrate index changes, the operating range is somewhat away from the desired aqueous environment. In order to shift the location of the minimum relative output power, a dielectric overlay was added on the top of the Au-coated ARROW-B SPR sensor as shown in Fig. 5. The resonant refractive indices of the superstrate when the resonant coupling occurs with and without the dielectric overlay are governed by the following equation[9]:

$$\sqrt{\frac{\epsilon_{mr}\, n_{\mathrm{SPR},0}^2}{\epsilon_{mr}+n_{\mathrm{SPR},0}^2}} = \sqrt{\frac{\epsilon_{mr}\, n_{\mathrm{SPR},1}^2}{\epsilon_{mr}+n_{\mathrm{SPR},1}^2}} + \frac{2\pi}{\lambda}\frac{n_{\mathrm{SPR},1}}{\sqrt{-\epsilon_{mr}}}\,(n_f^2 - n_{\mathrm{SPR},1}^2)\,d_f, \tag{7}$$

where $n_{\mathrm{SPR},0}$ and $n_{\mathrm{SPR},1}$ denote the superstrate indices without and with the dielectric overlay, respectively. ϵ_{mr} is the real part of the relative permittivity of the metal, and n_f and d_f are the refractive index and the thickness of the dielectric overlay, respectively.

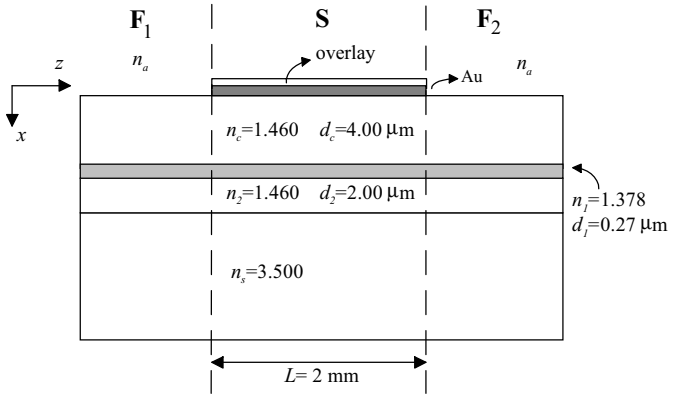

Figure 5. An Au-coated ARROW-B SPR sensor with an overlay.

Recall that the superstrate index at the minimum output power for $d_m = 35$ nm is around 1.370. By replacing $n_{\mathrm{SPR},0}$ with 1.370 and $n_{\mathrm{SPR},1}$ with 1.332 (refractive index of water) into Eq. (7), the overlay thickness d_f, as a function of the overlay index n_f, can be calculated and is shown in Fig. 6(a). According to experimental investigations, materials like Al_2O_3, Y_2O_3,[9] Ta_2O_5,[10] etc., which have been successfully formed on the gold film, are proper candidates for the overlay. Here, Al_2O_3 was selected as the overlay material. By specifying $n_f = 1.650$ (the refractive index of Al_2O_3 at $\lambda = 0.6328$ μm), it can be found that the thickness of the Al_2O_3 overlay d_f corresponding to $n_{\mathrm{SPR},1} = 1.332$ is around 13.5 nm. To check out the effect of overlay tuning, Fig. 6(b) shows relative output powers as functions of the superstrate index for $d_f = 12$, 18 nm, and without overlay.

To optimize the Au-coated ARROW-B SPR sensor in aqueous environment, the sensing resolution or minimum detectable change in the superstrate index n_a used as a measure can be defined as[11]

$$|\delta n_{min}| = \left| \frac{M\; p(L)}{\frac{\partial\, p(L)}{\partial\, n}} \right|_{n=n_a}, \tag{8}$$

where $p(L)$ is the relative output power defined as Eq. (6), and M is the measurement precision of $p(L)$ as a percentage (typically, 1%[9]).

Fig. 7(a) and (b) show the relative output power versus superstrate index for different overlay thicknesses. Based on the result, the minimum detectable changes $|\delta n_{min}|$ can be calculated and are shown in Table. 1. Among these cases, it's obvious that the one with $d_f = 14$ nm has the smallest sensing resolution of 5.56×10^{-5}, and hence the highest sensitivity. Fig. 8 shows the relative output power curve for this optimized ARROW-B SPR sensor.

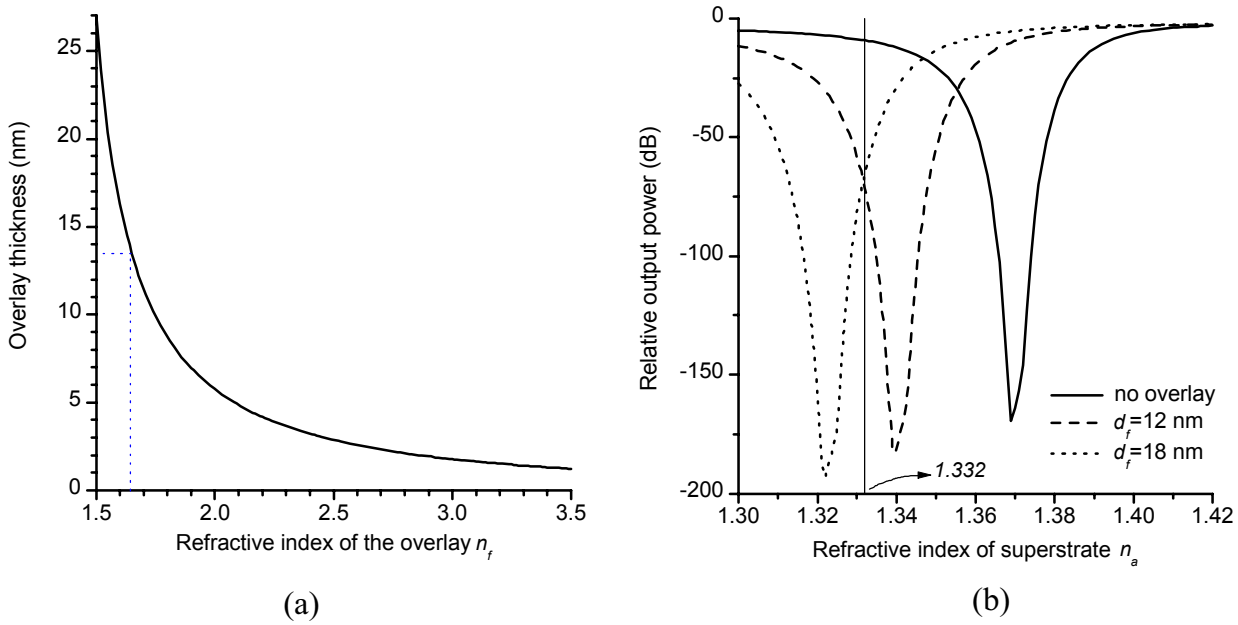

Figure 6. (a) Overlay thickness versus the refractive index of the overlay for nspr=1.332. (b) Dependence of the relative output power on the superstrate index.

Table 1. Sensing resolution for various overlay thicknesses.

overlay thickness	12 nm	13 nm	14 nm	15 nm	16 nm	17 nm	18 nm
resolution $\lvert\delta n_{min}\rvert$	8.50×10^{-5}	7.15×10^{-5}	5.56×10^{-5}	1.04×10^{-4}	6.53×10^{-5}	8.25×10^{-5}	9.73×10^{-5}

The resolution of our device is 5.56×10^{-5} using power measurement. Compared with a conventional waveguide SPR sensor, which also works in aqueous environment but uses "wavelength" measurement, having resolution $\sim 6 \times 10^{-5}$,[10] it seems that our ARROW-B SPR sensor is quite competitive with the conventional waveguide. As for the prism SPR sensor and the grating SPR sensor with optical power resolution of 0.2% have resolutions of 5×10^{-5} and 2×10^{-4}, respectively.[1] To change our 1% optical power resolution into 0.2%, our device resolution becomes 1.11×10^{-5}, which shows better sensing ability than these two configurations.

5. SUMMARY

An ARROW-B SPR sensor operating in aqueous environment has been investigated. The characteristics of ARROW-B waveguides and surface plasmon waves are briefly discussed. The design methodology including the selection of material and thickness of the metal layer is given. In addition to a design example of an Au-coated ARROW-B SPR sensor, the method of overlay tuning which can effectively shift the operating range to the desired environment is also presented. By optimizing the sensor with an Al_2O_3 overlay, the minimum detectable change in environment index is of the order of 10^{-5}, which is better than or comparable to previous conventional waveguide, prism, and grating SPR sensors. In addition, the design of an ARROW SPR sensor for detecting H_2 molecules with Pd as the metal film will also be discussed.

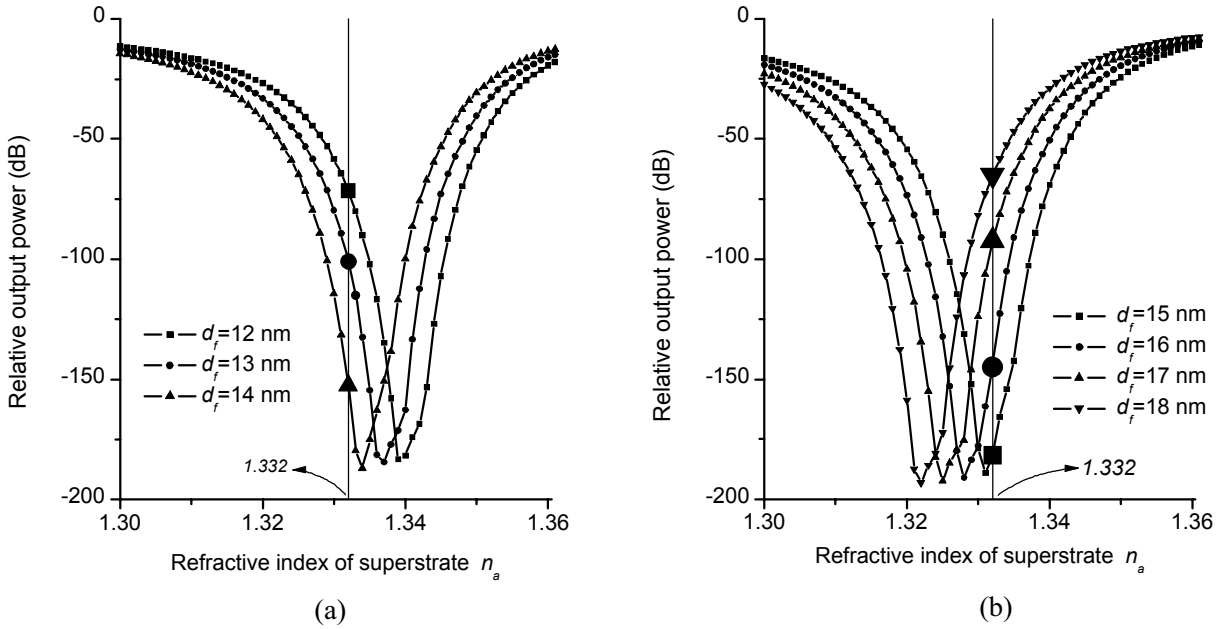

Figure 7. Relative output power versus superstrate index for various overlay thicknesses.

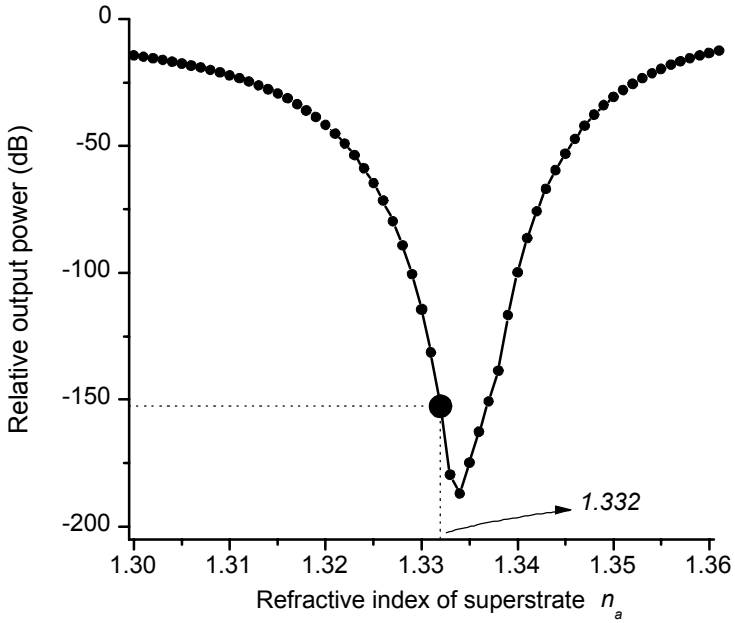

Figure 8. Relative output power versus superstrate index for an optimized Au-coated ARROW-B SPR sensor.

ACKNOWLEDGMENTS

This work was supported by the National Science Council of the Republic of China under contract NSC89-2215-E-009-079.

REFERENCES

1. J. Homola, S. S. Yee, and G. Gauglitz, "Surface plasmon resonance sensors: review," *Sensors and Actuators B*, vol. 54, pp. 3–15, 1999.
2. R. D. Harris and J. S. Wilkinson, "Waveguide surface plasmon resonance sensors," *Sensors and Actuators B*, vol. 29, pp. 261–267, 1995.
3. M. A. Duguay, Y. Kokubun, T. L. Koch, and L. Pfeiffer, "Antiresonant reflecting optical waveguides in SiO_2–Si multilayer structures," *Appl. Phys. Lett.*, vol. 49, no. 1, pp. 13–15, 1986.
4. T. Baba and Y. Kokubun, "New polarization-insensitive antiresonant reflecting optical waveguide (ARROW–B)," *IEEE Photon. Technol. Lett.*, vol. 1, no. 8, pp. 232–234, 1989.
5. T. Baba and Y. Kokubun, "Dispersion and radiation loss characteristics of antiresonant reflecting optical waveguides — numerical results and analytical expressions," *IEEE J. of Quantum Electron.*, vol. 28, no. 7, pp. 1689–1700, 1992.
6. H. Raether, *Surface Plasmons*, Springer-Verlag, 1988.
7. H. E. de Bruijn, R. P. H. Kooyman, and J. Greve, "Choice of metal and wavelength for surface-plasmon resonance sensors: some considerations," *Appl. Opt.*, vol. 31, no. 4, pp. 440–442, 1992.
8. *Surface plasmon resonance biosensors*, http://www.biosensor.com/bio/plasm.htm.
9. J. Homola, J. Ctyroky, M. Skalsky, J. Hradilova, and P. Kolarova, "A surface plasmon resonance based integrated optical sensor," *Sensors and Actuators B*, vol. 38–39, pp. 286–290, 1997.
10. J. Ctyroky, J. Homola, and M. Skalsky, "Tuning of spectral operation range of a waveguide surface plasmon resonance sensor," *Electron. Lett.*, vol. 33, pp. 1246–1248, 1997.
11. M. N. Weiss, R. Srivastava, H. Groger, P. Lo, and S. F. Luo, "A theoretical investigation of environmental monitoring using surface plasmon resonance waveguide sensors," *Sensors and Actuators A*, vol. 51, pp. 211–217, 1996.